Performance of a Low-Cost Earthquake Early Warning System (P-Alert) during the 2016 M_L 6.4 Meinong (Taiwan) Earthquake

by Yih-Min Wu, Wen-Tzong Liang, Himanshu Mittal, Wei-An Chao, Cheng-Horng Lin, Bor-Shouh Huang, and Che-Min Lin

ABSTRACT

On 5 February 2016, a moderate earthquake occurred in southwestern Taiwan with M_L 6.4 and a focal depth of 16.7 km. This earthquake caused damage to a few buildings and 117 casualties. A low-cost earthquake early warning (EEW) system (*P*-alert) is in operation for the purpose of EEW and for providing near-real-time shake maps. During this event, a detailed shaking map was generated by the *P*-alert system within 2 min after the earthquake occurrence, and the high shaking regions strongly correlated with the locations in which the damage and casualties occurred. In the field, individual *P*-alert devices also serve as onsite EEW systems using *P*-wave information. The individual *P*-alert provided a 4–8 s lead time before the arrival of violent shaking in the damaged regions. For regional EEW, both the Central Weather Bureau (CWB, official agency) and the *P*-alert system responded very well. Currently, regional warnings in Taiwan are only provided to cities at epicentral distances of 50 km or more by the CWB. For cities within a 50-km epicentral distance, the *P*-alert system could be useful for providing onsite EEW. The performance of the *P*-alert network during this earthquake proves the efficiency of this real-time, low-cost network in terms of early warning (regional and onsite), near-real-time shake maps, rapid reports, and strong-motion data for research purposes.

INTRODUCTION

Taiwan is perhaps one of the most seismically active regions in the world due to the collision of the Eurasian plate (EP) and the Philippine Sea plate (PSP; Tsai *et al.*, 1977; Wu *et al.*, 2008) and is continuously threatened by large and devastating earthquakes. Numerous earthquakes of magnitude 4 and above occur every year inland and off the east coast of Taiwan island. Some damaging events have inflicted severe casualties and property losses. These earthquakes can be divided into those associated with the northward subduction of the PSP under the EP and those associated with active faults in western Taiwan (Wu *et al.*, 1999).

From the viewpoint of regional seismotectonics, the recent moderate earthquake on 5 February 2016 could be associated with earthquakes in the second category occurring on active faults in western Taiwan. According to the source parameters issued by the Central Weather Bureau (CWB) rapid reporting system (Wu *et al.*, 1997, 2000), the earthquake was located in the Meinong District of Kaohsiung city, ~28 km northeast of Pingtung City in southern Taiwan (Fig. 1) at a focal depth of 16.7 km. The focal mechanism of this event has been reported by the Broadband Array in Taiwan for Seismology (BATS) and the U.S. Geological Survey (USGS), both of which suggest a

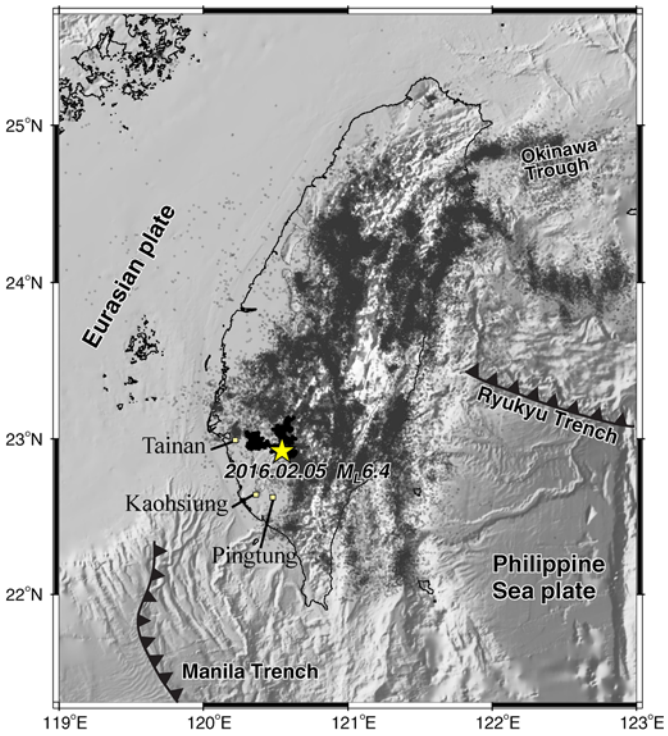

▲ **Figure 1.** The tectonic setup of Taiwan. The star depicts the epicenter of the earthquake event on 5 February 2016. The color version of this figure is available only in the electronic edition.

 doi: 10.1785/0220160058

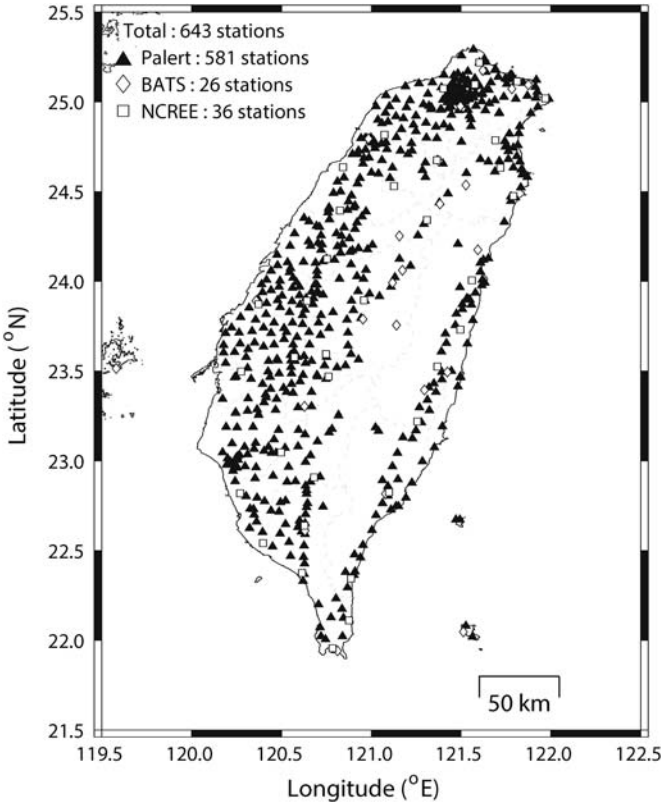

▲ **Figure 2.** Station distribution of the *P*-alert and Broadband Array in Taiwan for Seismology (BATS) and National Center for Research on Earthquake Engineering (NCREE) real-time strong-motion networks.

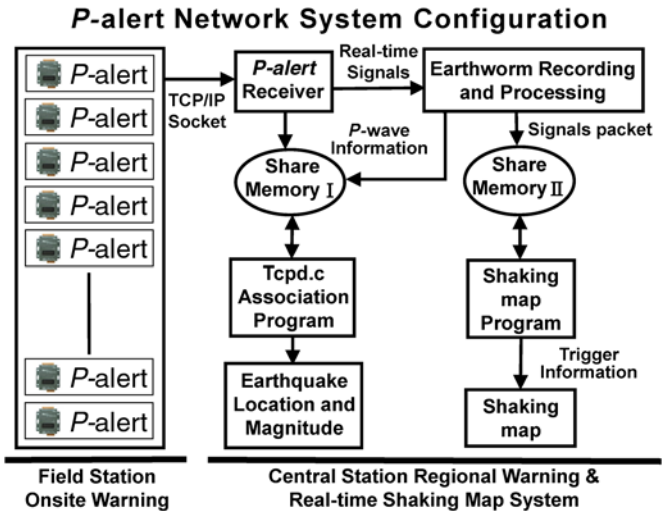

▲ **Figure 3.** Configuration of the *P*-alert real-time strong-motion network. The color version of this figure is available only in the electronic edition.

thrust mechanism with two nodal planes striking in the north–south (NS) and the northwest–southeast (NW–SE) directions. This earthquake caused heavy shaking in southwestern Taiwan and the maximum intensity reached 7 (peak ground acceleration [PGA] > 400 Gal) as recorded by a EEW system (*P*-alert) seismic network, which is the highest intensity on the seismic intensity scale of the CWB (Wu *et al.*, 2003). This event caused widespread building damage, soil liquefaction, and 117 casualties around the Tainan and Kaohsiung regions. Consequently, it is the most damaging event in the Taiwan region since the 1999 Chi-Chi earthquake (Chang *et al.*, 2000, 2007; Shin and Teng, 2001; Chen *et al.*, 2012). A low-cost *P*-alert seismic network developed by the National Taiwan University (NTU) with 581 microelectromechanical system (MEMS) accelerometers is in operation (Wu *et al.*, 2013; Wu, 2015). During this event, the *P*-alert network recorded high-quality strong-motion signals and produced detailed shaking maps within 2 min of the occurrence of the earthquake. The high shaking regions of the *P*-alert intensity map strongly correlated with the locations in which the damage and casualty occurred. In addition, this system shows the potential to identify rupture directivity, which is one of the key indexes used to estimate possible damage (Hsieh *et al.*, 2014; Wu, 2015). Individual *P*-alert devices also serve as an onsite EEW system. These devices provide an alert when the *P*-wave vertical displacement amplitude exceeds 0.35 cm or PGA > 80 Gal

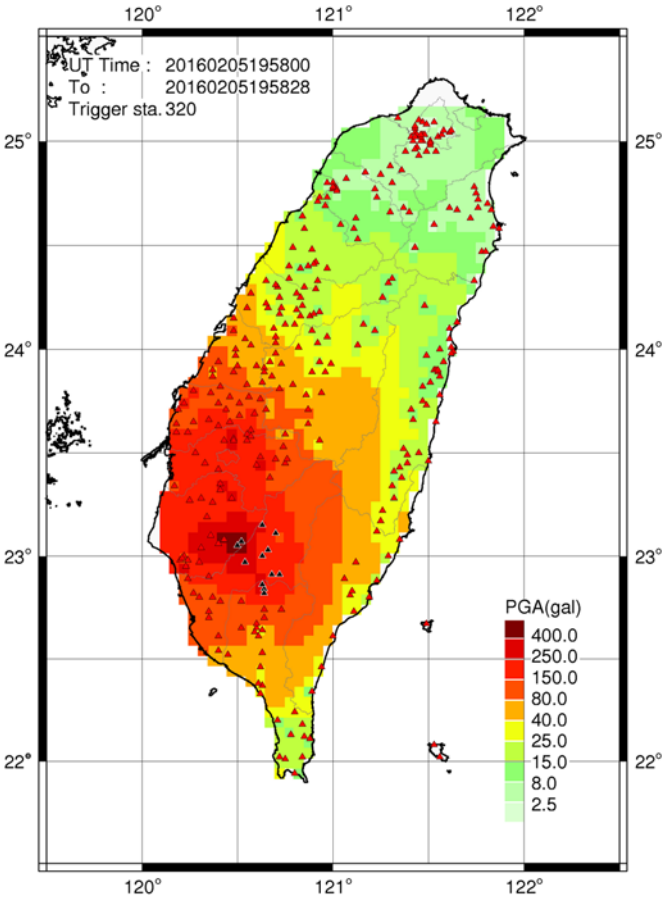

▲ **Figure 4.** Shake map of the 5 February 2016 M_L 6.4 Meinong earthquake produced and delivered by the *P*-alert network. The black triangles represent the 12 stations that were initially triggered and provided the shake map. The color version of this figure is available only in the electronic edition.

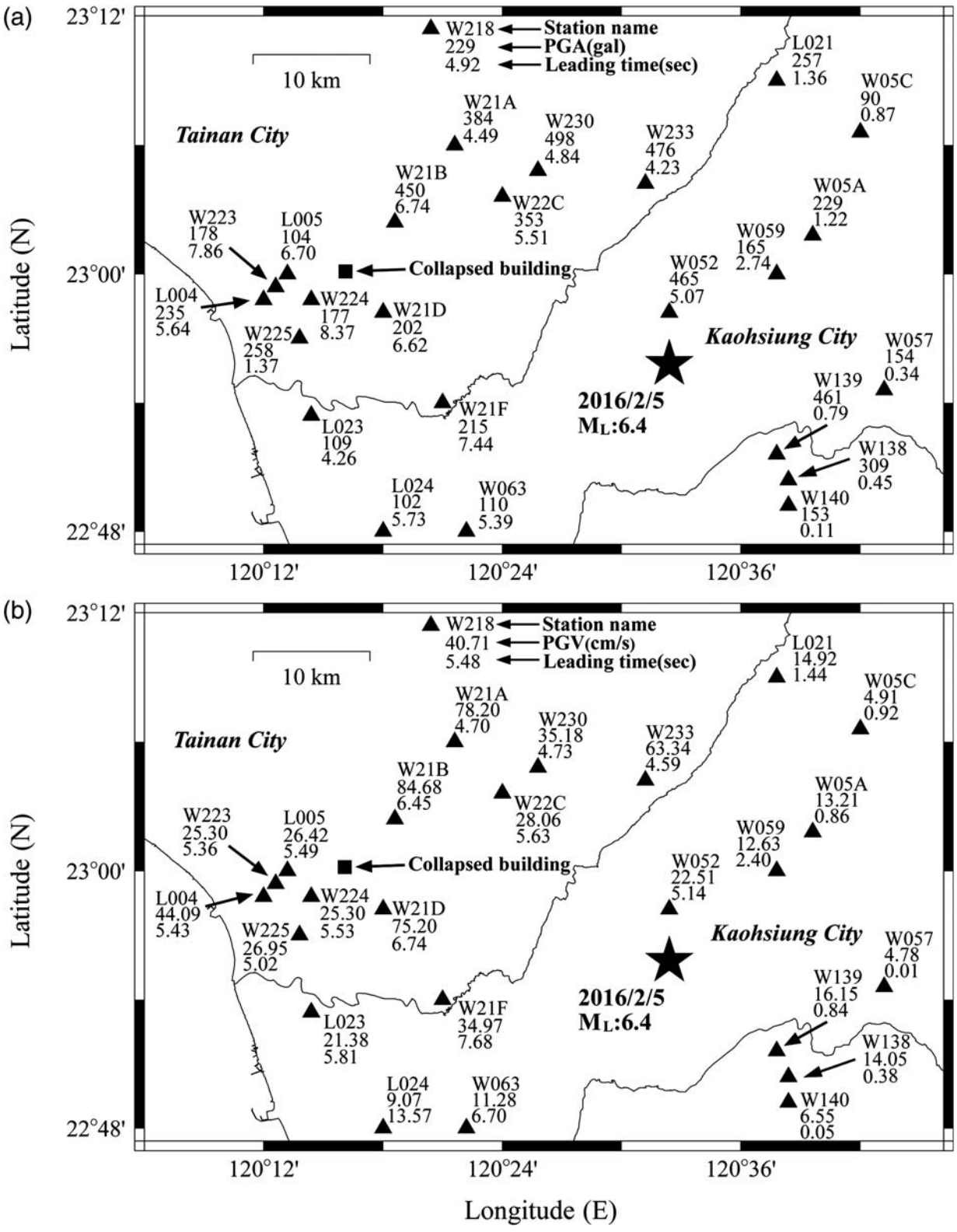

▲ **Figure 5.** Early warning lead times for *P*-alert stations in regions close to the epicenters of the 5 February 2016 M_L 6.4 Meinong, Taiwan, earthquakes. (a) Lead time and peak ground acceleration (PGA) for different stations. (b) Lead time and peak ground velocity (PGV) for different stations. Lead time is defined as the interval between the time when the filtered vertical displacement exceeds 0.35 cm or acceleration is larger than 80 Gal and the time of PGA and PGV.

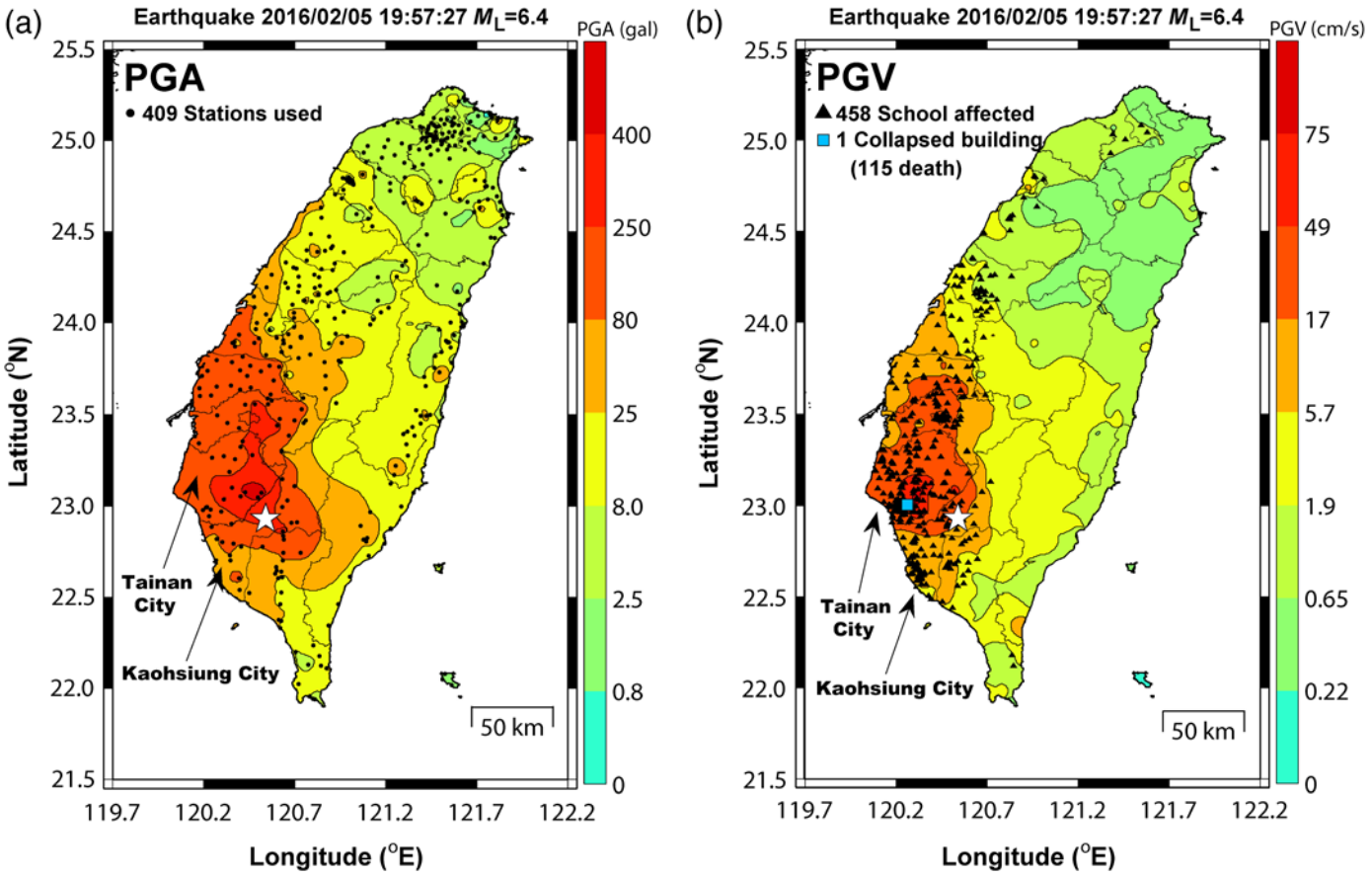

▲ **Figure 6.** (a) Shake map of the PGA from *P*-alert, BATS, and NCREE real-time strong-motion networks. (b) Shake map of PGV. The triangles and square in the PGV map show the distribution of schools affected and a fully collapsed building that caused 115 casualties as reported by National Science and Technology Center for Disaster Reduction (NCDR), respectively. The color version of this figure is available only in the electronic edition.

(Wu *et al.*, 2011, 2013; Hsieh *et al.*, 2015). In this study, we explore the performance and results of this high-density low-cost strong-motion network.

P-ALERT NETWORK

MEMS accelerometers were introduced to seismic applications in the early 1990s (Holland, 2003). These small and low-cost sensors have proven to be efficient for recording strong ground motion shaking. Taking advantage of MEMS technology, a research group at NTU, along with a private organization, developed a MEMS accelerometer *P*-alert system that is specially designed for EEW. With the support of the Ministry of Science and Technology (MOST) of Taiwan, NTU initiated a pilot experiment in 2010 and installed a seismic network with 15 MEMS *P*-alert accelerometers in eastern Taiwan (Wu and Lin, 2014). Encouraged by the functionality and ability of these small MEMS devices to record earthquakes in Taiwan, this network was extended to other areas of Taiwan (Wu *et al.*, 2013; Wu, 2015). Currently, 581 *P*-alert stations have been installed all over the country. Most of these stations are located in elementary schools where adequate power and Internet connections are provided. Data from these *P*-alert systems are transferred continuously to a central processing station. Along with the *P*-alert stations, real-time strong-motion signals from 26 stations of BATS (Institute of Earth Sciences, Academia Sinica, Taiwan, 1996) and 36 stations of the National Center for Research on Earthquake Engineering (NCREE) are also received by the *P*-alert central recording station. Figure 2 shows the station distribution of the *P*-alert, BATS, and NCREE networks.

The configuration of the *P*-alert network is shown in Figure 3. Each *P*-alert device is equipped with a three-component accelerometer with 16-bit resolution and a $\pm 2g$ full dynamic range. The sampling rate is 100 samples per second. The frequency band is from d.c. to 10 Hz. According to the software algorithm embedded in the *P*-alert, the signal from each field station is processed for the detection of *P*-wave arrivals and is continuously double integrated into the displacement signal for calculating the vertical peak amplitude of displacement from the *P* wave, *Pd* (Wu and Kanamori, 2005). Once the captured signal exceeds the predefined thresholds, the *P*-alert device sends an alert with a warning sound for onsite EEW purposes. As previously stated, *P*-alert has the capability to act both as an onsite EEW system and a regional EEW system.

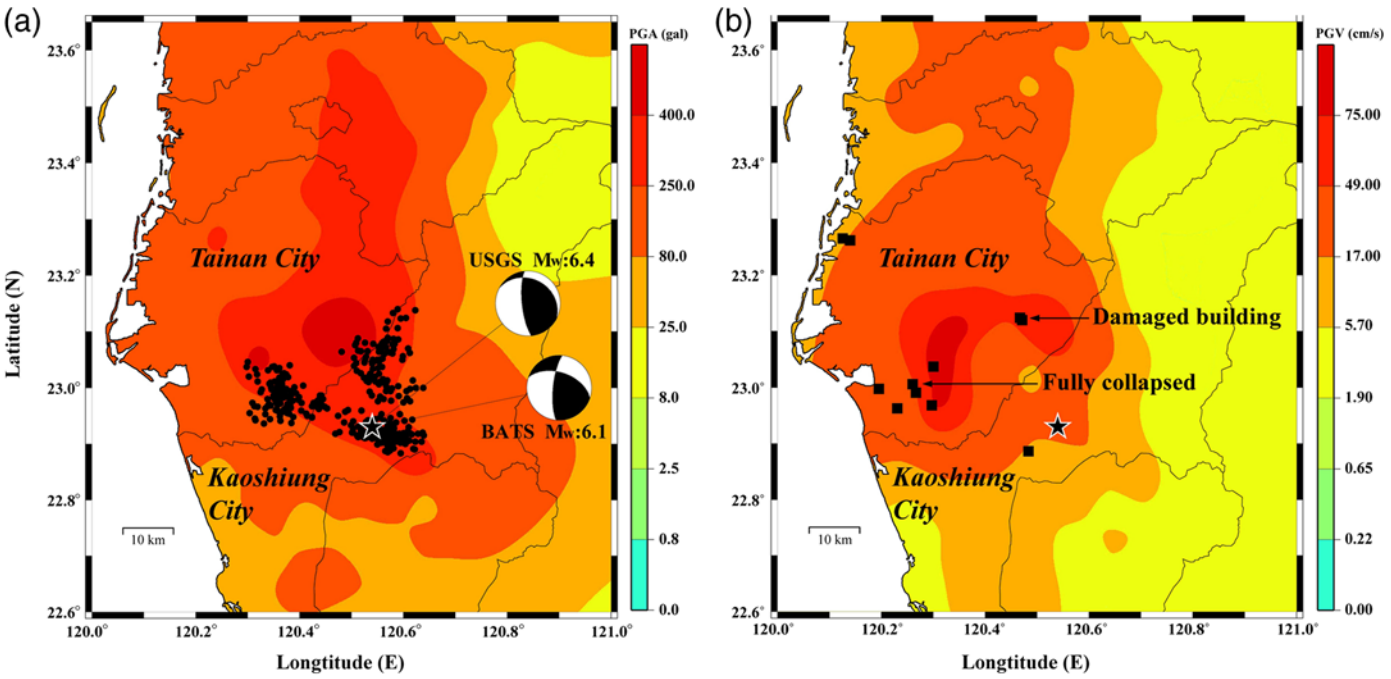

▲ **Figure 7.** (a) PGA shake map of earthquake source regions and focal mechanisms and aftershock distribution of the 2016 Meinong earthquake reported by the Central Weather Bureau (CWB). (b) PGV shake map of earthquake source regions. Solid squares show the sites of the structurally damaged buildings. Most of these buildings are located in the areas where PGV > 17 cm/s. The color version of this figure is available only in the electronic edition.

For the purpose of regional EEW system, signals are delivered via the Internet to a central station and are then processed in a real-time system using EarthWorm software (Johnson *et al.*, 1995; Chen *et al.*, 2015). The real-time signals are also processed for generating a near-real-time shake map (Wu *et al.*, 2013; Hsieh *et al.*, 2014; Wu, 2015).

Presently, an official regional EEW message in Taiwan is delivered by the CWB. The regional EEW process using the *P*-alert network is only used for research purposes. During the 2016 Meinong earthquake, the CWB and *P*-alert systems provided EEW information 12 s and 15 s, respectively, after the earthquake occurrence with estimated magnitudes of 6.1 and 6.2, respectively. Both of these systems responded well as regional EEW systems. However, the *P*-alert system required time because the minimum number of stations to trigger the threshold is set at 12 to obtain better station coverage of the dense array in operation, which is much larger than that of the CWB system.

NEAR-REAL-TIME SHAKE MAP

The *P*-alert network is capable of providing near-real-time shake maps using strong-motion signals. In the *P*-alert central station, whenever 12 stations detect PGA higher than 1.2 Gal, the system will produce a shake map. One to three minutes after the system is triggered, these shake maps are delivered via e-mail to specific users (including the National Science and Technology Center for Disaster Reduction [NCDR]) every minute. Figure 4 shows the shake map of the 2016 Meinong earthquake delivered by the *P*-alert system along with the initially triggered 12 instruments responsible for producing the shake map. Forty-two minutes after the earthquake, this shake map was also posted on social networks for research purposes.

The CWB system generates a very sparse shake map with a limited number of stations. However, with a dense array in operation, the shake map from the *P*-alert system provides much more detailed shaking conditions. For example, the CWB reported that Tainan city was the most damaged region, where shaking intensity reached 5 (PGA < 250 Gal; see Data and Resources). However, most of the *P*-alert stations in the eastern portion of Tainan city observed a PGA higher than 250 Gal, and three stations showed a PGA larger than 400 Gal. Approximately 2 weeks after the occurrence of the earthquake, the CWB reported an intensity of 7 (PGA > 400 Gal) in the eastern portion of Tainan city. Clearly, an operationally dense array is needed, and low-cost sensors are useful for this purpose.

ONSITE EEW

Currently, the CWB can provide a regional EEW message ~15 s after an earthquake occurs (Chen *et al.*, 2015). In addition, the CWB is capable of providing early warning to cities located at distances more than 50 km from the epicenter. However, epicentral distances less than 50 km are blind zones for the regional EEW system in Taiwan. To overcome this problem, individual *P*-alert devices are installed in the blind zones to provide onsite EEW alerts. The *P*-alert device sends an alert when the *Pd* or PGA is greater than 0.35 cm or 80 Gal,

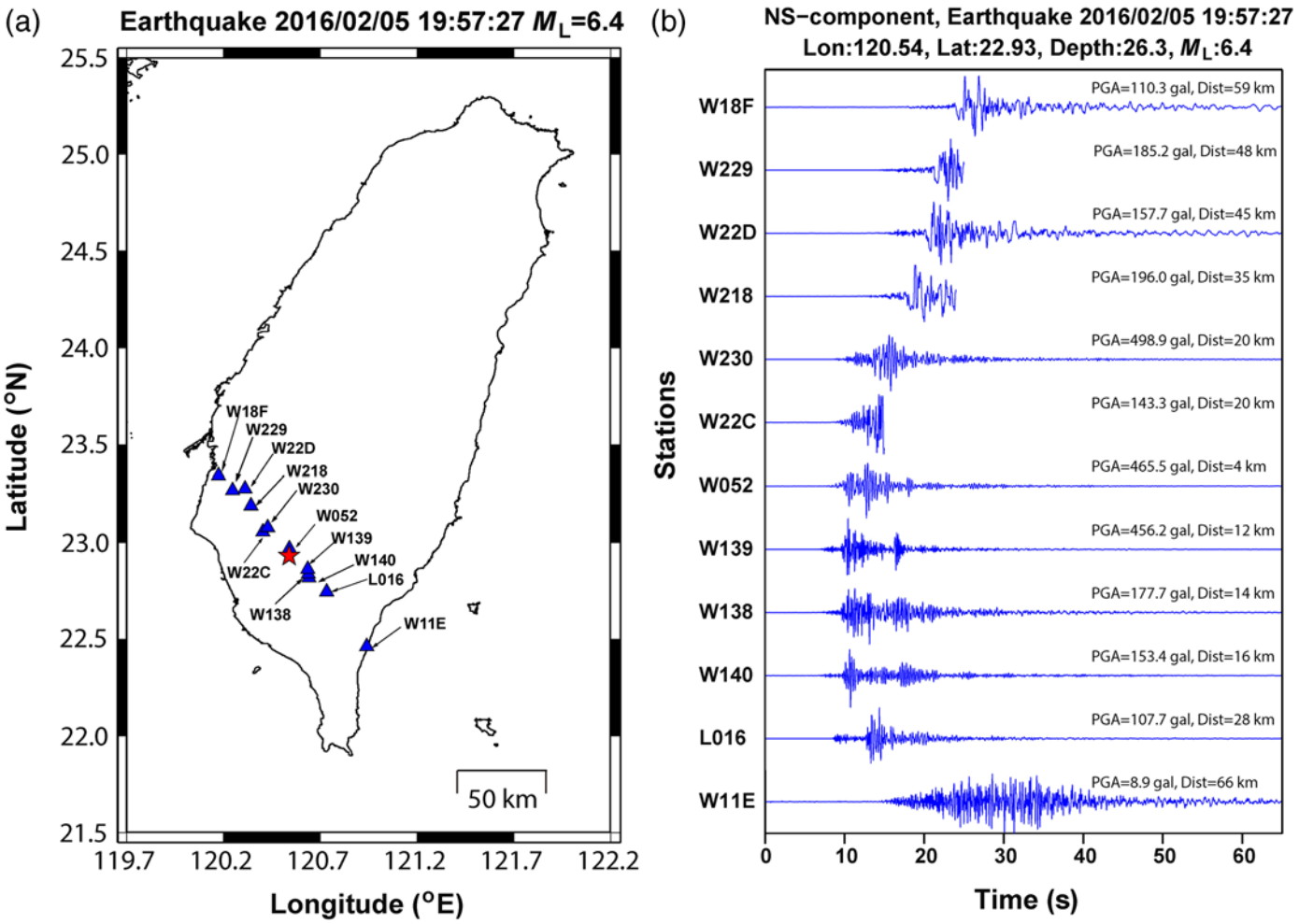

▲ **Figure 8.** (a) A profile showing the possible rupture direction. (b) Near-epicentral strong-motion records of the 5 February 2016 M_L 6.4 Meinong earthquake recorded by the *P*-alert network. A few stations could not send data to the central stations, which commonly occurs after the arrival of *S* waves. The color version of this figure is available only in the electronic edition.

respectively. Figure 5 shows the resulting early warning lead times near epicentral regions for the 2016 Meinong earthquake. The early warning lead time is defined as the interval between the time when the filtered vertical displacement exceeds 0.35 cm or accelerations are larger than 80 Gal and the time of the PGA or peak ground velocity (PGV). Obviously, for the most damaged regions in Tainan city, the *P*-alert onsite method can provide approximately 5–8 s lead time before the arrival of PGA or PGV.

DISCUSSION AND CONCLUSIONS

The 2016 Meinong earthquake provided an excellent opportunity to examine the functionality of the *P*-alert network in Taiwan. Timely shake maps deliver valuable information for assessing damage patterns. Figure 6 shows the PGA and PGV shake maps from *P*-alert, BATS, and NCREE networks, whereas Figure 6b shows the distribution of the schools affected by the 2016 Meinong earthquake (National Science and Technology Center for Disaster Reduction, 2016). Most of the schools affected have nonstructural damage due to reinforcement after the 1999 Chi-Chi earthquake (Tsai and Hwang, 2008; Chung *et al.*, 2014). Only three of the schools are structurally damaged. By comparing the shake maps and distribution of the affected schools, it is obvious that the damage pattern is in agreement with the shake map provided by the *P*-alert system. Most of the affected schools and collapsed buildings occurred in areas of high PGV (i.e., >17 cm/s). The most affected region is Tainan city, where maximum shaking (497 Gal) was observed. In total, 113 schools were damaged in the Tainan area. The second most affected city was Kaohsiung where 47 schools were damaged. This earthquake caused a building to collapse, which claimed 115 fatalities, in a location (square in Fig. 6b) close to the high PGA and PGV region.

The shake maps are not only helpful for damage assessment, but also they can be used for identification of the direction of the earthquake source rupture as documented in

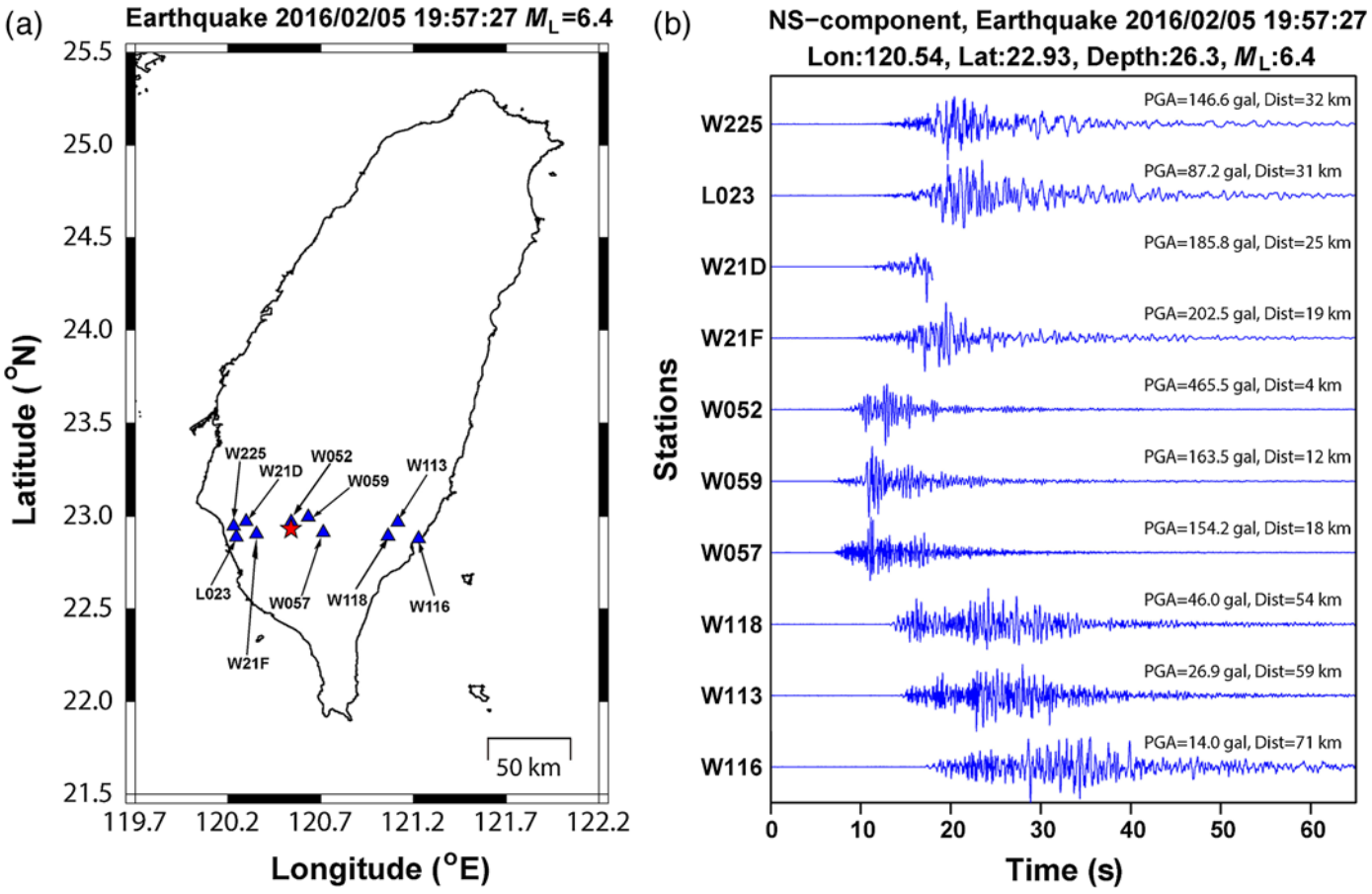

▲ **Figure 9.** (a) Another profile to show the quality of the data recorded by the *P*-alert network. (b) North–south (NS) component of strong-motion records of all the instruments shown in (a). The color version of this figure is available only in the electronic edition.

previous studies (e.g., Hsieh *et al.*, 2014; Wu, 2015). The location, shake map, and focal mechanisms of this earthquake were obtained only a few minutes to tens of minutes after the earthquake occurrence (Fig. 7). Based on the focal mechanism solutions from the USGS and BATS, the two nodal fault planes have strikes about NW–SE and NS. According to the epicenter and shake map results, the high PGA and PGV regions are located on the northwestern side of the epicenter. Obviously, the fault plane may be NW–SE, and the source may have ruptured northwestward. Figure 7 also shows the aftershock distribution. Most of the aftershocks are located toward the western side of the epicenter, which confirms the NW–SE fault plane, and could be the reason that this earthquake produced the highest shaking in Tainan city. On one hand, it can be stated that source effects play a major role. On the other hand, most of Tainan city is located on sedimentary plains that enhance shaking. The rupture pattern of the 2016 Meinong earthquake is similar to the 2010 M_w 6.3 Jiasiang earthquake (Huang *et al.*, 2011; Lee *et al.*, 2013). Solid squares in Figure 7 show the locations of 11 structurally damaged buildings identified by NCREE. The geographical distribution of the damaged buildings is in agreement with the PGV shake map, because most of the buildings are located in regions where the PGV is larger than 17 cm/s. It is worth noting that the distribution of the aftershock sequence is much more coherent with the high PGA pattern. However, the distribution of the structurally damaged buildings is much closer to the high PGV pattern. As discussed in our previous studies (Wu *et al.*, 2004), the PGV may be a better indicator of damage than the PGA during this earthquake.

Approximately 10 hours after the earthquake occurrence, strong-motion data from 373 *P*-alert stations were released to seismologists for research purposes. Figure 8 shows the strong-motion records of the 2016 Meinong earthquake from the *P*-alert network that were recorded at stations distributed in a NW–SE fashion away from the epicenter. Clearly, stations located in the NW direction observed higher shaking, whereas relatively less shaking was observed in the SE direction, which again confirms the possible rupture direction. Figure 9 shows additional strong-motion records to show the quality of the waveform recorded by the *P*-alert network. Some of the stations could not send data to the central stations after the arrival of the *S* waves, which may be attributed to short interruptions of both power and the Internet during and after the strong shaking. However, this phenomenon does not affect the functionality of the EEW system, because the *P*-alert EEW system uses *P*-wave information that was not affected. During this event, only ~2% of the *P*-alert stations could not transfer

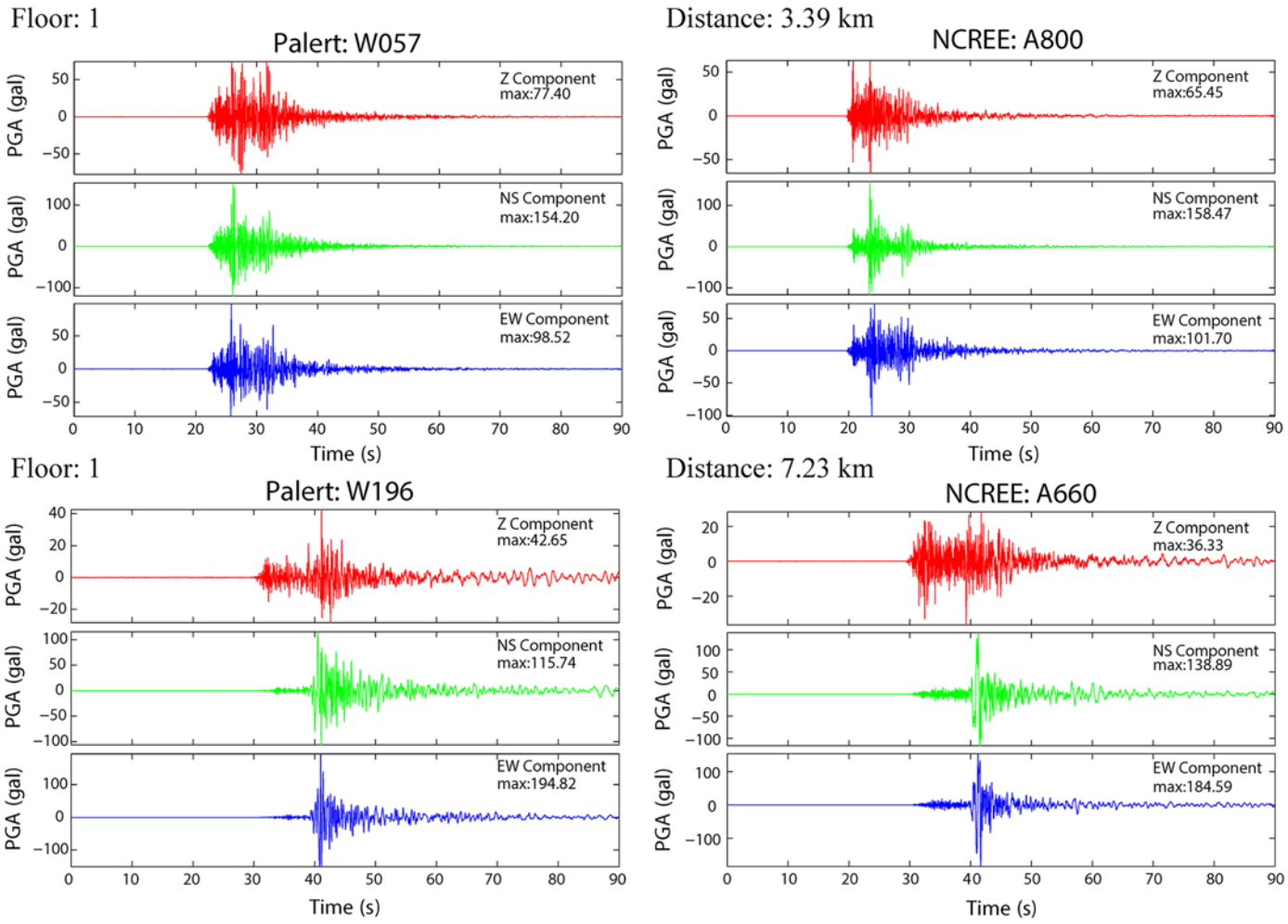

▲ **Figure 10.** A comparison of waveform recording by *P*-alert and NCREE stations. In the first case, the distance between the two types of instruments is 3.39 km, whereas in the latter case it is 7.23 km. The color version of this figure is available only in the electronic edition.

complete signals to the central station after the *S*-wave arrival. However, *P*-wave information from those stations can still be used, and the other stations kept the system smoothly in operation (Wu *et al.* 2013; Hsieh *et al.*, 2014). Some *P*-alert instruments are located in close proximity to the NCREE instruments, which provides a good platform to compare the data quality recorded by this low-cost network. Figure 10 shows the comparison between both types of instruments.

The low-cost MEMS sensors provide not only strong-motion records but also provide insight about useful information that can be extracted from this dense array in operation. For example, if we take a closer look at the waveforms, as shown in Figure 8, two strong *S*-wave pulses are observed at the northwestern stations, which is unusual. These two strong *S*-wave pulses may come from source or path effects. In the present work, we do not intend to go into detail about this observation; however, the Seismic Analysis Code (SAC; see Data and Resources) format of the strong-motion records (unit in Gal, polarity positive in vertical, north, and east, and frequency band of *P*-alert is from d.c. to 10 Hz) can be downloaded from the NTU cloud disk (see Data and Resources) and can be used for further studies. A table in the compressed file provides the station information of the *P*-alert network (see Data and Resources).

In conclusion, the 2016 Meinong earthquake provided a useful platform to test the functionality of the *P*-alert network. For the onsite EEW system, it provided an example of EEW system with the *P*-wave method. A central processing station provides shake map information a few minutes after the earthquake occurrence. Approximately 10 hours after the earthquake occurrence, strong-motion data were disseminated to the seismology community for research purposes. The performance of the *P*-alert network during this earthquake proves the efficiency of this real-time, low-cost MEMS sensor network in terms of early warning, rapid reporting, and strong-motion data for research purposes. This dense array is possible due to its relatively low cost. However, the low signal-to-noise ratio of the *P*-alert device only focuses on large event observations, and signals recorded by the NTU *P*-alert network may include building responses; therefore, it could be improved in the future.

DATA AND RESOURCES

The strong-motion waveform records used in this study were obtained from the National Taiwan University (NTU), the Institute of Earth Sciences (IES) of Academia Sinica, and National Center for Research on Earthquake Engineering (NCREE) of Taiwan. The *P*-alert records used in this study are available to the public and can be downloaded from the NTU cloud disk (https://www.space.ntu.edu.tw/navigate/s/5CDFA7C2CFD7487FB84E2CE3F7376C33QQY, last accessed February 2016). The strong-motion records from IES and NCREE used in this study can be obtained upon request from IES and NCREE. The damage records used in this study can also be obtained upon request from NCREE and the National Science and Technology Center for Disaster Reduction (NCDR) of Taiwan. Broadband Array in Taiwan for Seismology (BATS) Centroid Moment Tensor (CMT) solutions are available at http://bats.earth.sinica.edu.tw, and U.S. Geological Survey (USGS) CMT solutions are maintained at http://earthquake.usgs.gov/earthquakes. Central Weather Bureau (CWB) website can be accessed at http://www.cwb.gov.tw/eng/index.htm (last accessed February 2016). Seismic Analysis Code (SAC) is available at http://ds.iris.edu/files/sac-manual/ (last accessed July 2016).

ACKNOWLEDGMENTS

This research was supported by the Ministry of Science and Technology (MOST) of Taiwan (MOST-104-2116-M-002-016). We thank the Central Weather Bureau, Taiwan, for providing seismic records. The comments from two anonymous reviewers and associate editor helped in improving the article. The author gratefully acknowledges Wessel and Smith (1998) for the Generic Mapping Tool (GMT) software that was used in plotting some of the figures. We also would like to thank Chia-Hua Hsieh and Benjamin M. Yang for maintaining the *P*-alert network.

REFERENCES

Chang, C. H., Y. M. Wu, T. C. Shin, and C. Y. Wang (2000). Relocating the 1999 Chi-Chi earthquake, Taiwan, *Terr. Atmos. Ocean. Sci.* **11,** 581–590.

Chang, C. H., Y. M. Wu, L. Zhao, and F. T. Wu (2007). Aftershocks of the 1999 Chi-Chi, Taiwan, earthquake: The first hour, *Bull. Seismol. Soc. Am.* **97,** 1245–1258, doi: 10.1785/0120060184.

Chen, D. Y., N. C. Hsiao, and Y. M. Wu (2015). The Earthworm based earthquake alarm reporting system in Taiwan, *Bull. Seismol. Soc. Am.* **105,** 568–579, doi: 10.1785/0120140147.

Chen, D. Y., T. L. Lin, Y. M. Wu, and N. C. Hsiao (2012). Testing a *P*-wave earthquake early warning system by simulating the 1999 Chi-Chi, Taiwan, M_w 7.6 earthquake, *Seismol. Res. Lett.* **83,** 103–108, doi: 10.1785/gssrl.83.1.103.

Chung, L. L., Y. S. Yang, K. H. Lien, and L. Y. Wu (2014). In situ experiment on retrofit of school buildings by adding sandwich columns to partition brick walls, *Earthq. Eng. Struct. Dynam.* **43,** 339–355, doi: 10.1002/eqe.2347.

Holland, A. (2003). Earthquake data recorded by the MEMS accelerometer: Field testing in Idaho, *Seismol. Res. Lett.* **74,** 20–26, doi: 10.1785/gssrl.74.1.20.

Hsieh, C. Y., W. A. Chao, and Y. M. Wu (2015). An examination of the threshold-based earthquake early warning approach using a low cost seismic network, *Seismol. Res. Lett.* **86,** 1664–1667, doi: 10.1785/0220150073.

Hsieh, C. Y., Y. M. Wu, T. L. Chin, K. H. Kuo, D. Y. Chen, K. S. Wang, Y. T. Chan, W. Y. Chang, W. S. Li, and S. H. Ker (2014). Low cost seismic network practical applications for producing quick shaking maps in Taiwan, *Terr. Atmos. Ocean. Sci.* **25,** 617–624, doi: 10.3319/TAO.2014.03.27.01(T).

Huang, H. H., Y. M. Wu, T. L. Lin, W. A. Chao, J. B. H. Shyu, C. H. Chan, and C. H. Chang (2011). The preliminary study of the 4 March 2010 M_w 6.3 Jiasian, Taiwan, earthquake sequence, *Terr. Atmos. Ocean. Sci.* **22,** 283–290, doi: 10.3319/TAO.2010.12.13.01(T).

Institute of Earth Sciences, Academia Sinica, Taiwan (1996). *Broadband array in Taiwan for seismology*. Institute of Earth Sciences, Academia Sinica, Taiwan, Other/Seismic Network, doi: 10.7914/SN/TW.

Johnson, C. E., A. Bittenbinder, B. Bogaert, L. Dietz, and W. Kohler (1995). Earthworm: A flexible approach to seismic network processing, *Incorporated Research Institutions for Seismology Newsletter*, **14,** no. 2, 1–4, http://www.iris.iris.edu/newsletter/FallNewsletter/earthworm.html (last accessed March 2016).

Lee, S. J., W. T. Liang, L. Mozziconacci, Y. J. Hsu, W. G. Huang, and B. S. Huang (2013). Source complexity of the 4 March 2010 Jiashian, Taiwan earthquake determined by joint inversion of teleseismic and near field data, *J. Asian Earth Sci.* **64,** 14–26, doi: 10.1016/j.jseaes.2012.11.018.

National Science and Technology Center for Disaster Reduction (2016). *Summary of the Damages Caused by 2016 Meinong Earthquake*, http://www.ncdr.nat.gov.tw/EarthquakeMeinong1050206.aspx (last accessed March 2016).

Shin, T. C., and T. L. Teng (2001). An overview of the 1999 Chi-Chi, Taiwan, earthquake, *Bull. Seismol. Soc. Am.* **91,** 895–913.

Tsai, K. C., and S. J. Hwang (2008). Seismic retrofit program for Taiwan school buildings after 1999 Chi-Chi earthquake, in *The 14th World Conference on Earthquake Engineering*, Beijing, China, 12–17 October.

Tsai, Y. B., T. L. Teng, J. M. Chiu, and H. L. Liu (1977). Tectonic implications of the seismicity in the Taiwan region, *Mem. Geol. Soc. China* **2,** 13–41.

Wessel, P., and W. H. F. Smith (1998). New, improved version of generic mapping tools released, *Eos Trans. AGU* **79,** 579, doi: 10.1029/98EO00426.

Wu, Y. M. (2015). Progress on development of an earthquake early warning system using low cost sensors, *Pure Appl. Geophys.* **172,** 2343–2351, doi: 10.1007/s00024-014-0933-5.

Wu, Y. M., and H. Kanamori (2005). Rapid assessment of damaging potential of earthquakes in Taiwan from the beginning of *P*-waves, *Bull. Seismol. Soc. Am.* **95,** 1181–1185, doi: 10.1785/0120040193.

Wu, Y. M., and T. L. Lin (2014). A test of earthquake early warning system using low cost accelerometer in Hualien, Taiwan, in *Early Warning for Geological Disasters - Scientific Methods and Current Practice*, F. Wenzel and J. Zschau (Editors), Springer, Berlin, 253–261, ISBN: 978-3-642-12232-3, doi: 10.1007/978-3-642-12233-0_13.

Wu, Y. M., C. H. Chang, L. Zhao, T. L. Teng, and M. Nakamura (2008). A comprehensive relocation of earthquakes in Taiwan from 1991 to 2005, *Bull. Seismol. Soc. Am.* **98,** 1471–1481, doi: 10.1785/0120070166.

Wu, Y. M., D. Y. Chen, T. L. Lin, C. Y. Hsieh, T. L. Chin, W. Y. Chang, W. S. Li, and S. H. Ker (2013). A high-density seismic network for earthquake early warning in Taiwan based on low cost sensors, *Seismol. Res. Lett.* **84,** 1048–1054, doi: 10.1785/0220130085.

Wu, Y. M., C. C. Chen, T. C. Shin, Y. B. Tsai, W. H. K. Lee, and T. L. Teng (1997). Taiwan rapid earthquake information release system, *Seismol. Res. Lett.* **68,** 931–943.

Wu, Y. M., J. K. Chung, T. C. Shin, N. C. Hsiao, Y. B. Tsai, W. H. K. Lee, and T. L. Teng (1999). Development of an integrated earthquake early warning system in Taiwan—Case for Hualien earthquakes, *Terr. Atmos. Ocean. Sci.* **10,** 719–736.

Wu, Y. M., N. C. Hsiao, and T. L. Teng (2004). Relationships between strong ground motion peak values and seismic loss during the 1999 Chi-Chi, Taiwan earthquake, *Nat. Hazards* **32,** 357–373.

Wu, Y. M., W. H. K. Lee, C. C. Chen, T. C. Shin, T. L. Teng, and Y. B. Tsai (2000). Performance of the Taiwan Rapid Earthquake Information Release System (RTD) during the 1999 Chi-Chi (Taiwan) earthquake, *Seismol. Res. Lett.* **71,** 338–343.

Wu, Y. M., T. L. Lin, W. A. Chao, H. H. Huang, N. C. Hsiao, and C. H. Chang (2011). Faster short-distance earthquake early warning using continued monitoring of filtered vertical displacement—A case study for the 2010 Jiasian earthquake, Taiwan, *Bull. Seismol. Soc. Am.* **101,** 701–709, doi: 10.1785/0120100153.

Wu, Y. M., T. L. Teng, T. C. Shin, and N. C. Hsiao (2003). Relationship between peak ground acceleration, peak ground velocity, and intensity in Taiwan, *Bull. Seismol. Soc. Am.* **93,** 386–396.

Yih-Min Wu[1]
Himanshu Mittal
Wei-An Chao
Department of Geosciences
National Taiwan University
1 Roosevelt Road Section 4
Taipei 10617, Taiwan
drymwu@ntu.edu.tw

Wen-Tzong Liang
Cheng-Horng Lin[1,2]
Bor-Shouh Huang[2]
Institute of Earth Sciences
Academia Sinica
128 Academia Road Section 2
Taipei 11529, Taiwan

Che-Min Lin
National Center for Research on Earthquake Engineering
National Applied Research Laboratories
200 Hsin-Hai Road Section 3
Taipei 10668, Taiwan

Published Online 3 August 2016

[1] Also at National Center for Research on Earthquake Engineering, National Applied Research Laboratories, 200 Hsin-Hai Road Section 3, Taipei 10668, Taiwan.

[2] Also at Department of Geosciences, National Taiwan University, 1 Roosevelt Road Section 4, Taipei 10617, Taiwan.